Estuarine, Coastal and Shelf Science 188 (2017) 163–173

Contents lists available at ScienceDirect

Estuarine, Coastal and Shelf Science

journal homepage: www.elsevier.com/locate/ecss

Successive impact of tidal bores on sedimentary processes: Arcins channel, Garonne River

David Reungoat [a, b], Xinqian Leng [c], Hubert Chanson [c, *]

[a] Université de Bordeaux, I2M, Laboratoire TREFLE, 16 Avenue Pey-Berland, Pessac, France
[b] CNRS UMR 5295, 33607 Pessac, France
[c] The University of Queensland, School of Civil Engineering, Brisbane, QLD 4072, Australia

ARTICLE INFO

Article history:
Received 22 December 2016
Received in revised form
24 January 2017
Accepted 21 February 2017
Available online 22 February 2017

Keywords:
Tidal bore
Sedimentary processes
Suspended sediments
Field observations
Garonne River

ABSTRACT

A tidal bore is a hydrodynamic shock, propagating upstream as the tidal flow turns to rising, with macro-tidal conditions in a funnel shaped system with shallow waters. The tidal bore of the Garonne River was extensively investigated in the Arcins channel between 2010 and 2013, typically over one to two days. In 2015, new field measurements were repeated systematically at the same site on 29 August-1 September 2015 and on 27 October 2015. The nature of the observations was comprehensive, encompassing hydrodynamics and turbulence, as well as sediment properties and transport. The tidal bore occurrence had a marked effect on the velocity and suspended sediment field, including a rapid flow deceleration and flow reversal during the bore passage, with very large suspended sediment concentrations (SSCs) during the passage of the tidal bore front and early flood tide, as well as very large suspended sediment flux during the very early flood tide. The suspended sediment concentration (SSC) data indicated a gradual increase in initial mean SSC estimate prior to the bore from 29 August to 1 September 2015. A comparison between suspended sediment flux data showed very significant suspended sediment flux on the first day of tidal bore occurrence, with a decreasing magnitude over the next three days. The data suggested a two-stage bed scour process: at each tidal bore event, surface erosion occurred initially, in the form of stripping; the first stage was followed by delayed mass erosion, occurring about 5–15 min after the tidal bore.

1. Introduction

A tidal bore is a compressive wave of tidal origin, propagating upstream as the tidal flow turns to rising (Fig. 1). It might be observed when a macro-tidal flood flow enters a funnel shaped river mouth with shallow waters (Stoker, 1957; Tricker, 1965). The occurrence of tidal bores has a significant impact on the natural systems (Chen et al., 1990; Simpson et al., 2004; Wolanski et al., 2004). Their impact on sedimentary processes was documented in the field and in laboratory (Bartsch-Winkler et al., 1985; Faas, 1995; Khezri and Chanson, 2012). It is understood that the bore propagation is associated with intense sediment scouring and suspension of bed materials (Greb and Archer, 2007; Khezri and Chanson, 2015; Furgerot et al., 2016) (Fig. 1A). The tidal bore passage may also contribute to channel shifting in flat and wide shallow-water systems (Chanson, 2011). The very early flood flow is characterised by very high suspended sediment concentrations (Chanson et al., 2011; Furgerot et al., 2013; Fan et al., 2014). In cohesive sediment river systems, the erosional processes are linked to the rheological properties of sediment deposits, and field observations suggest that the bore passage induces some initial surface erosion and bed liquefaction, followed by delayed bulk erosion (Tessier and Terwindt, 1994; Faas, 1995; Keevil et al., 2015).

The tidal bore of the Garonne River (France) was extensively investigated in the Arcins channel in 2010, 2012 and 2013 with a focus on hydrodynamic and suspended sediment processes (Chanson et al., 2011; Reungoat et al., 2014, 2015, Keevil et al., 2015). Each study was conducted over one to two days, providing a snapshot based upon a single bore event. In the present study, field measurements were repeatedly conducted over a four-day period, and the comprehensive nature of the observations encompassed hydrodynamics and turbulence, sedimentology and transport. The aim of the study was to comprehend the temporal evolution of hydrodynamics and sediment characteristics in a tidal-bore

* Corresponding author.
E-mail address: h.chanson@uq.edu.au (H. Chanson).

http://dx.doi.org/10.1016/j.ecss.2017.02.025
0272-7714/

Fig. 1. Photographs of tidal bores - Bore propagation from left to right (see arrow). (A) Breaking tidal bore of the Qiantang River (China) in the northern channel about Daquekou on 6 September 2013 - Note the black colour of the bore front - Bore propagation from bottom left to top right (see arrow). (B) Undular tidal bore of the Dordogne River (France) at Port de Saint Pardon on 2 September 2015 morning - Note the early morning fog in the background - This site is located 20 km NE of the Arcins channel sampling site and the tidal bore arrives at Port de Saint Pardon about 30 min after it reached the Arcins channel.

affected estuary during a spring tide period. New field measurements were repeated systematically on 29 August, 30 August, 31 August and 1 September 2015, and on 27 October 2015 nearly 8 weeks later, during a dry period with low river discharges. Continuous velocity measurements collected at high-frequency (200 Hz) were complemented by a careful characterisation of the sediment materials collected.

2. Methods

2.1. Field site and instrumentation

The field measurements were performed in the Arcins channel of the Garonne River (France), close to Lastrene, at the same site previously used by Chanson et al. (2011), Reungoat et al. (2014), and Keevil et al. (2015). The channel is 1.8 km long, 70 m wide and about 1.1–2.5 m deep at low tide (Fig. 2). Cross-sectional surveys were conducted on each day and typical results are presented in Fig. 2C, with z being the vertical elevation in m NGF IGN69. In Fig. 2C, the data are compared to the 2013 bathymetric survey data at the same location (The 2010, 2012, 2013 and 2015 surveys were all conducted at the same cross-section). The bathymetry results as well as visual observations tended to indicate a progressive siltation of the Arcins channel at the sampling site since 2012, including further siltation along the right bank since 2013. The tide data showed a semi-diurnal trend, with slightly different periods and amplitudes typical of some diurnal inequality. The complete field measurements were conducted under spring tide conditions between 29 August and 1 September 2015, and on 27 October 2015, while additional observations were performed on 28 August 2015, 26 October and 28 October 2015. A summary of the tidal conditions is listed in Table 1 (column 3). Present measurements were performed at the end of a relatively dry summer period with low Garonne River levels.

The free surface elevations were measured manually using a survey staff, located about 2 m away from the velocimeter to minimise any interference. During each tidal bore passage, the water level was recorded using a HD video camera Sony™ HDR PJ200E for about 10–15 min. The instantaneous velocity components were recorded with a Nortek™ acoustic Doppler velocimeter (ADV) Vectrino+ (10 MHz), equipped with a down-looking ADV field head. The ADV unit was fixed beneath a hull of a heavy and sturdy pontoon and Fig. 2A and C shows the ADV location. The control volume was located 1.0 m below the free-surface (Fig. 2C). The ADV settings included a velocity range of 2.5 m/s, a transmit length of 0.3 mm and a sampling volume of 1.5 mm height; the ADV power setting was High-on 29 August, 31 August, 1 September 2015 and 27 October 2015, and Low on 30 August 2015. The power setting was selected after preliminary tests, to optimise the acoustic backscatter response of the ADV unit with the Garonne River sediment (Reungoat et al., 2016). The ADV unit was sampled continuously at 200 Hz, starting at least 1 h prior to the bore passage and extending at least 1 h after the tidal bore. All the ADV data underwent a rigorous post-processing procedure to eliminate any erroneous and corrupted data (Reungoat et al., 2016). The percentage of good samples ranged between 60% and 90% for the entire data sets.

2.2. Sediment characterisation

Sediment bed materials and sediment-laden water samples were collected in the Arcins channel on 27, 29, 30 and 31 August, 1 September 2015, and on 27 and 28 October 2015. Bed materials were taken at the end of ebb tide, next to the right bank waterline. Water samples were collected prior to and shortly after the tidal bore about 0.1 m below the water surface. The bed samples were characterised in laboratory: i.e., rheometry and backscatter tests. Both water sample sediments and bed sediments were further tested for the material density and granulometry. The granulometry tests were conducted using a Malvern™ laser Mastersizer 2000 equipped with a Hydro 3000SM dispersion unit for wet samples. The rheological properties of bed material samples were tested with two rheometers: a rheometer Anton Paar™ Physica MR301 equipped with a plane-cone CP50-SB6055 (= 50 mm, cone angle: 2°, truncation gap: 207 μm) and a rheometer Malvern™ Kinexus Pro (Serial MAL1031375) equipped with a plane-cone (= 40 mm, cone angle: 4°, truncation gap truncation: 150 μm). All tests were performed under controlled strain rate at constant temperature (25 C). Prior to each rheological test, a small bed sediment sample was placed carefully between the plate and cone, then subjected to a controlled strain rate loading and unloading between 0.01 s^{-1} and 1000 s^{-1} with a continuous ramp in each direction.

The calibration of the ADV unit was accomplished by measuring the ADV signal amplitude of known, artificially produced concentrations of material obtained from the bed, diluted in tap water and thoroughly mixed. The laboratory experiments were performed using the same Nortek™ ADV Vectrino + system with the same settings as for the field measurements. For each test, a known mass of wet sediment was introduced in a water tank which was continuously stirred with two mixers. The mass of wet sediment was measured with a Mettler™ Type PM200 (Serial 86.1.06.627.9.2) balance. The ADV signals were post-processed using the same

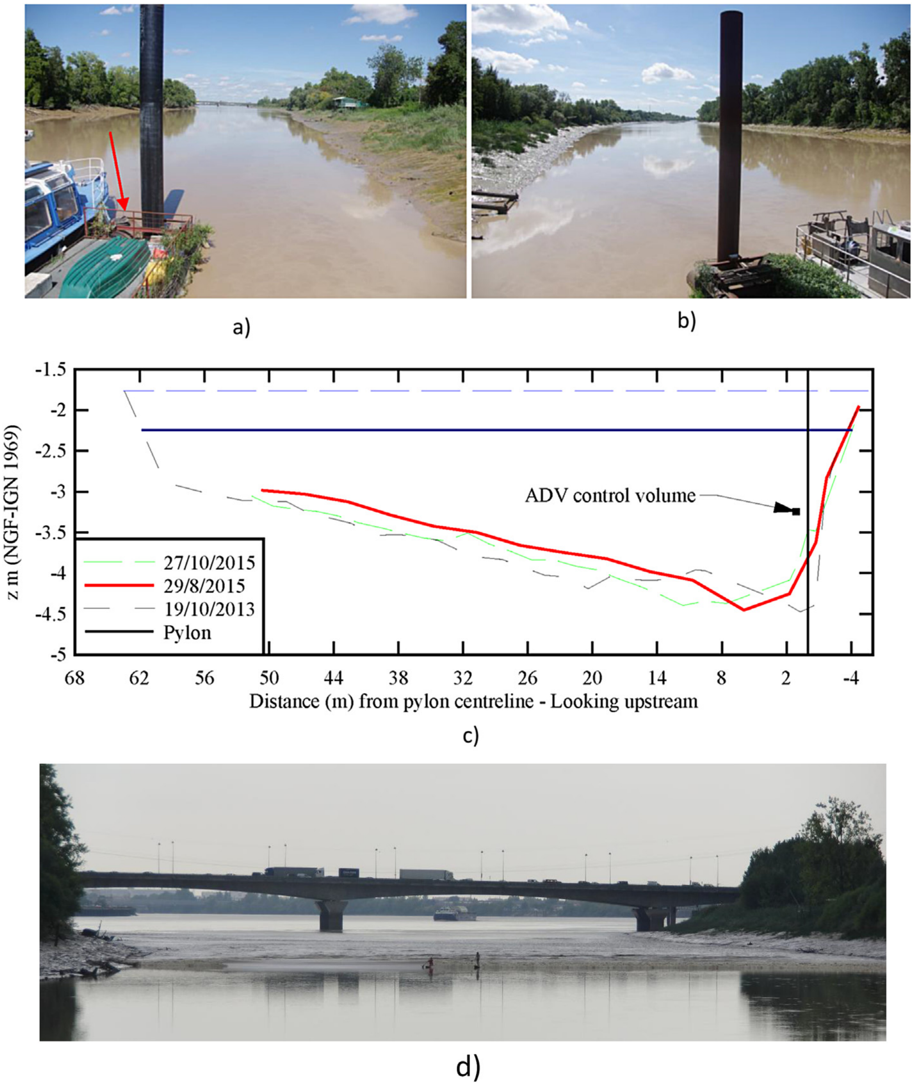

Fig. 2. Sampling site in the Arcins channel, Garonne River between Arcins Island and Latresne (France). (A, Left) Looking downstream (North) on 28 August 2015 during the ebb tide at 12:30, about 4 h before tidal bore - The red arrow points towards the ADV location. (B, Right) Looking upstream (South) from the pontoon on 28 August 2015 during the ebb tide at 12:30. (C) Surveyed distorted cross-sections on 29 August and 27 October 2015 looking downstream (i.e. North) - Comparison with the 2013 survey data at the same cross-section - Water levels immediately before (solid line) and after (dashed line) bore front are shown as well as ADV control volume before bore passage (black square) are shown for the 27 October 2015. (D) Tidal bore propagation in the northern end of the Arcins channel on 21 August 2015, looking dowsntream - Note the surfers for scale, and an Airbus barge in the background using the flood flow motion. (For interpretation of the references to colour in this figure legend, the reader is referred to the web version of this article.)

Table 1
Tidal bore observations in the Arcins channel, Garonne River (France).

Reference	Date	Tidal range ([1])	Fr_1	U (m/s)	A_1 (m^2)	B_1 (m)	a_w/L_w	T_w (s)
(1)	(2)	(3)	(4)	(5)	(6)	(7)	(8)	(9)
Present study	29/08/2015	5.85	1.18	4.23	101.4	67.6	0.0610	0.84
	30/08/2015	6.17	1.34	4.25	72.8	64.3	0.0727	0.90
	31/08/2015	6.22	1.70	1.79	56.6	65.1	0.0952	0.96
	01/09/2015	6.04	1.38	4.45	74.9	64.5	0.0980	0.99
	27/10/2015	6.32	1.33	4.61	88.0	65.9	0.0376	1.02
Keevil et al. (2015)	19/10/2013	6.09	1.27	4.32	85.6	65.0	0.0274	0.96
Reungoat et al. (2014)	7/06/2012	5.68	1.02	3.85	158.9	79.0	–	–
Chanson et al. (2011)	10/09/2010	6.03	1.30	4.49	105.7	75.4	0.0614	1.24
	11/09/2010	5.89	1.20	4.20	108.4	75.8	0.0470	1.28

Notes: ([1]): tidal range measured at Bordeaux, 8.4 km upstream of sampling location; Fr_1: tidal Froude number: $Fr_1 = (U + V_1)/(g \times A_1/B_1)^{1/2}$; U: tidal bore celerity at sampling site; A_1: initial cross-section area immediately prior to the tidal bore; B_1: initial free-surface width immediately prior to the tidal bore; a_w: undulation wave amplitude; L_w: undulation wave steepness; T_w: undulation wave period.

method as the field data: i.e., with the removal of communication errors, average signal to noise ratio data less than 5 dB, average correlation values less than 60%, and signal spikes based upon the phase-space thresholding technique.

2.3. Sediment properties

The dry sediment density was tested and the measurements yielded a relative density of 2.65. The relative density of wet sediment samples was $\mathbf{s} = 1.28$, from which a sample porosity of 0.84 was deduced. The particle size distribution data presented close results for all samples although they were collected over seven days at different locations and included both bed sediment and suspended sediment data (Fig. 3, Appendix I). The present results are compared to past observations in Appendix I.

The median particle size was 14 μm for both bed and suspended materials, corresponding to some silty material (Julien, 1995). The sorting coefficient $\sqrt{d_{90}/d_{10}}$ was about 3.8 for the bed materials and 4.1 for suspended sediments on average (Appendix I, column 8). The bed material consisted of about 10% clay, 88% silt and 2% sand, and the bed mixture presenting a narrower grain size distribution than the suspended sediments (Fig. 3A and B). Although the data set was limited, the results suggested little differences in sediment characteristics between water samples collected before and after the bore (Appendix I).

The sediment bed data may be compared with those of sediment materials at the same site in September 2010, June 2012 and October 2013 (Appendix I). The properties of the Garonne River bed sediment were similar between 2010 and 2015. The present data set however suggested a slight increase in median grain size and sorting coefficient with increasing time between 29 August and 1 September 2015. This is illustrated in Fig. 3C, presenting the evolution of characteristic grain sizes (d_{10}, d_{50} and d_{90}) over the four days of sampling. In situ, the bed sediment materials next to the waterline appeared to be softer than in previous field works. The surface mud layer was relatively fluid and seemed to become thinner from Saturday 29 August to Tuesday 1 September 2015. (No tidal bore was observed at the sampling site on 28 August 2015. From 29 August 2015, tidal bores occurred twice per day, although the field observations were conducted in the afternoon tidal bores

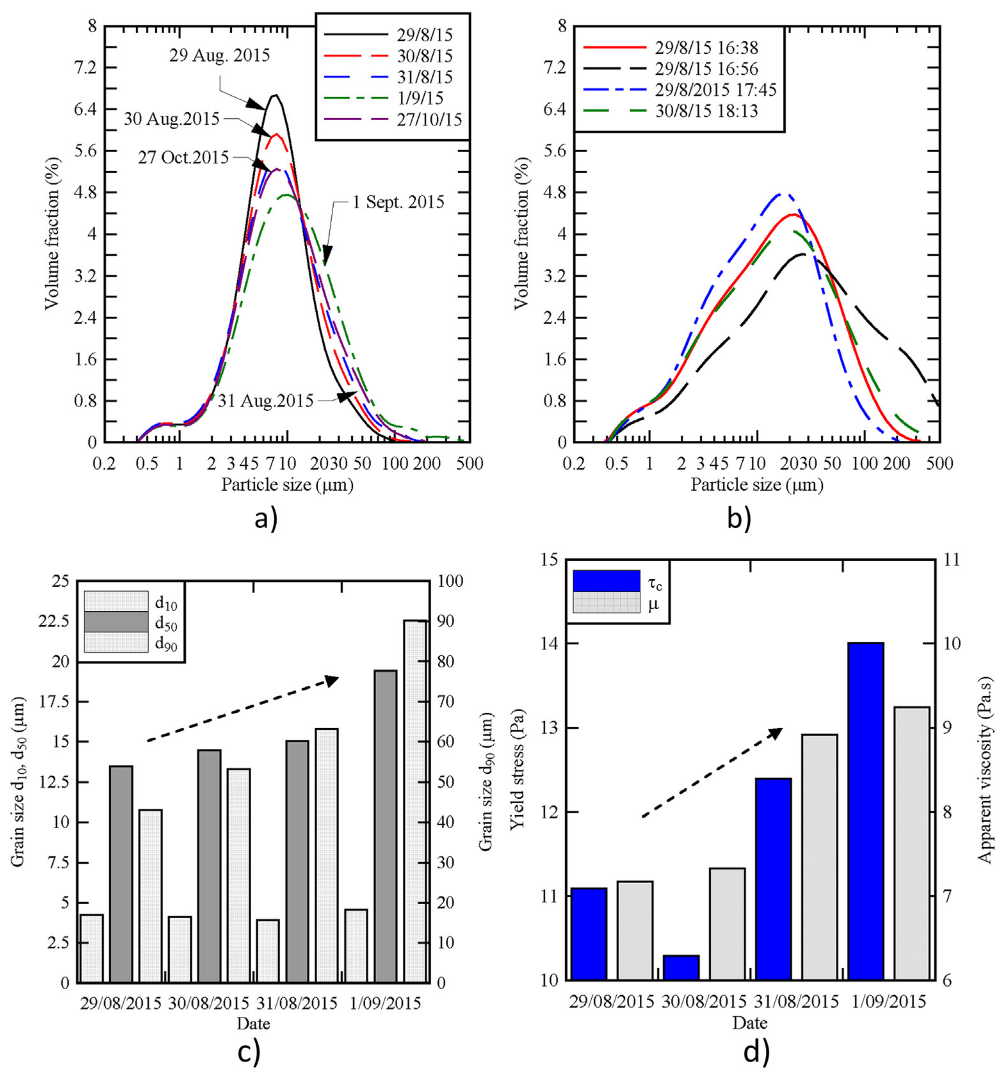

Fig. 3. Granulometry and rheometry characteristics of sediments collected in the Garonne River at Arcins between 29 August and 1 September 2015. (A, Left) Particle size distributions of sediment bed materials collected at end of ebb tide. (B, Right) Particle size distributions of suspended sediment samples collected after tidal bore - Tidal bore passage: 16:27 on 29 August 2015 and 17:15 on 30 August 2015. (C, Left) Evolution of characteristic grain size for sediment bed materials collected in the Arcins channel, Garonne River between 29 August and 1 September 2015, at end of ebb tide. (D, Right) Evolution of average apparent yield stress and effective viscosity of bed materials collected in the Arcins channel, Garonne River between 29 August and 1 September 2015.

only.) It was likely that the bed surface sediments were resuspended at each tidal bore and early flood tide, before redepositing during the late flood tide and ebb tide. The entire process might have contributed to some mixing between different sediments sources from various sections of the river, thus leading to a progressively broader grain size distribution associated with some increase in median sediment size.

On 27 October 2015, water sediment samples were collected before and after the tidal bore passage. For the first hour after the bore, the suspended sediment grain sizes were 50%–100% coarser than prior to the bore, although the sorting coefficient was nearly unchanged (Appendix I). After 100 min after the tidal bore passage, the sediment characteristics became closer to the ebb tide suspended sediment properties.

Rheometry tests provided quantitative informations on the relationship between shear stress and strain rate of the bed material. All data consistently indicated some difference between loading and unloading, typical of non-Newtonian thixotropic material, with the shear stress magnitude during unloading being consistently smaller than that during loading for a given shear rate. The rheometer data were used to estimate an apparent yield stress and viscosity (Appendix I). The yield stress and viscosity were derived by fitting the unloading rheometry data with a Herschel-Bulkley model, in line with earlier studies (Coussot, 1997; Roussel et al., 2004; Chanson et al., 2006; Keevil et al., 2015): $\tau = \tau_c + \mu \times (\partial V/\partial z)^m$, where τ is the shear stress, and $\partial V/\partial y$ is the shear strain rate. On average, the apparent viscosity was 8 Pa.s, the yield stress was about 12 Pa and m $\approx$ 0.28 for the bed sediment samples. The repeatability of the rheometry results was carefully checked by identically testing different samples; the results were very close (Reungoat et al., 2016). Present findings of yield stress τ_c ~12 Pa were comparable to previous investigations at the same site (Appendix I).

The results indicated a trend over the four days between 29 August and 1 September. The rheometry data showed some increase in yield stress and apparent viscosity (Appendix I). This is illustrated in Fig. 3D presenting the evolution of τ_c and μ over the four days. It is conceivable that the surface erosion during the tidal bore and early flood tide, and the subsequent deposition during the late flood tide and ebb tide, may have contributed to some mixing between sediments sources from different sections of the river, thus changing progressively the characteristic grain sizes, yield stress and apparent viscosity of the bed materials from 29 August to 1 September 2015 (Fig. 3C and D), as hinted by Lambiase (1980) and Faas (1995) in the Bay of Fundy.

2.4. Acoustic backscatter amplitude and suspended sediment concentration

The relationship between acoustic backscatter amplitude of ADV unit and suspended sediment concentration (SSC) was tested systematically for SSCs between 0 and 80 kg/m^3. The full data sets are presented in Reungoat et al. (2016), including a discussion on the ADV power setting effects. The data showed a monotonic increase in suspended sediment concentration with increasing signal amplitude for SSC less than 5–8 kg/m^3. For SSC >8 kg/m^3, the data showed a decreasing backscatter amplitude with increasing suspended sediment concentration. The general trends were consistent with a number of studies, including with cohesive sediment materials (Downing et al., 1995; Ha et al., 2009; Salehi and Strom, 2009; Guerrero et al., 2011; Chanson et al., 2011; Brown and Chanson, 2012; Keevil et al., 2015).

The sediment-laden water sample data analyses were compared further to the calibration data of the ADV unit (Fig. 4). The results presented a reasonable agreement between the measured SSCs and ADV backscatter readings, implying that the backscatter amplitude outputs may be used as a surrogate of SSC with the proper selection of some calibration curve.

All the field observations indicated that the suspended sediment concentrations were very low prior the tidal bore, while much larger sediment concentration levels were observed during and after the passage of the tidal bore (next section). Hence the SSC estimates were calculated using the following ADV calibration curves for SSC <8 kg/m^3:

$$SSC = \frac{-23913}{1 - 1.232 \times 10^7 \times e^{-0.0551 \times Ampl}} \quad SSC < 8\ kg\big/m^3 \ \ (Power = High-) \tag{1a}$$

$$SSC = \frac{-130.32}{1 - 2862 \times e^{-0.07793 \times Ampl}} \quad SSC < 8\ kg\big/m^3 \ \ (Power = low) \tag{1b}$$

where the backscatter amplitude (Ampl) is in counts, the suspended sediment concentration SSC is in kg/m^3, and Power refers to the ADV power settings: i.e., High- or Low. During and after the passage of the tidal bore, the SSCs were significantly larger and the ADV backscatter amplitude was attenuated by the heavily sediment-laden flow. The suspended sediment estimates were deduced from the ADV calibration data for SSC >8 kg/m^3:

$$SSC = 247.8 - 44.85 \times Ln(Ampl) \quad SSC < 8\ kg\big/m^3 \ \ (Power = High-) \tag{2a}$$

$$SSC = 191.0 - 39.91 \times Ln(Ampl) \quad SSC < 8\ kg\big/m^3 \ \ (Power = low) \tag{2b}$$

Equations (1) and (2) are compared to the calibration data in Fig. 4, as well as water sample data and the corresponding signal amplitude at time to collection. Equations (1) and (2) were applied to the field data set before and after the tidal bore passage respectively. The results are presented and discussed below.

3. Results

3.1. Hydrodynamics

The low tide slack and flow reversal were observed in the Arcins channel during the afternoons of 28, 29, 30 and 31 August, 1 September, and 26, 27 and 28 October 2015, although detailed measurements were only conducted on 29–31 August, 1 September and 27 October 2015 (Table 1). On 28 August 2015 afternoon, no tidal bore was observed: the early flood tide started with a rapid flow reversal, although without a discontinuity in terms of water depth. On all other days, a tidal bore formed at the northern end of the Arcins channel (Fig. 2D). As the bore propagated upstream, its shape evolved in response to bathymetric changes. The bore was undular at the sampling location, albeit some breaking was observed next to the left bank where the water was shallower. With the bore passage, the free-surface elevation rose very rapidly during the bore passage: i.e., by 0.3 m–0.5 m in the first 10–15 s (Fig. 5). The tidal bore propagated up to the southern end of the channel and the surfers could surf the bore for the entire Arcins channel length for nearly 8 min. On each day, the bore passage was followed by a series of strong whelps lasting for

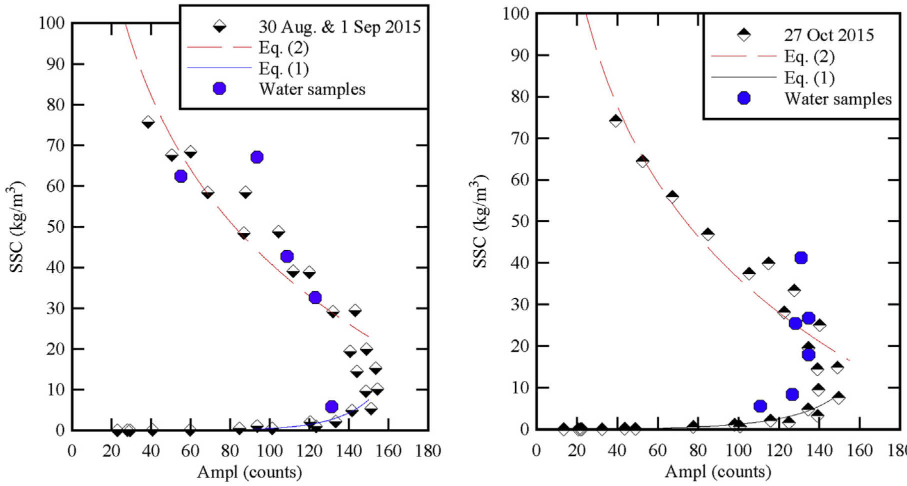

Fig. 4. Relationship between suspended sediment concentration (SSC) and ADV backscatter amplitude, including a comparison with sediment-laden water sample data - Mud samples and water samples collected on 30 August, 1 September and 27 October 2015.

several minutes. The wave period was about 1 s (Table 1, column 9).

The tidal bore shape is characterised its Froude number Fr_1 defined as:

$$Fr_1 = \frac{V_1 + U}{\sqrt{g \times \frac{A_1}{B_1}}} \tag{3}$$

where V_1 is the initial flow velocity positive downstream, U is the bore celerity positive upstream for a fixed observer, g is the gravity acceleration, A_1 is the initial flow cross-section area and B_1 is the initial free-surface width (Lighthill, 1978; Chanson, 2012). Based upon the survey data, the Froude numbers are summarised in Table 1: Fr_1 ranged from 1.2 to 1.7, consistent with the undular nature of the bore except on 31 August 2015. On 31 August 2015, the bore front was undular on the channel centreline and towards to the right bank, but breaking closer to the left bank. The characteristics of the secondary waves, called whelps or undulations, are summarised in Table 1 (columns 8 & 9).

Instantaneous velocity measurements were conducted continuously at high frequency prior to, during and after the tidal bore. Fig. 5 shows a typical data set, with the longitudinal velocity component V_x positive downstream towards Bordeaux, the transverse velocity component V_y positive towards the Arcins Island, and the vertical velocity component V_z positive upwards. In Fig. 5, the time-variations of the water depth are included as well as surface velocity data on the channel centre. Fig. 5D presents a close-up about the tidal bore passage time.

During the late ebb tide, the current velocity decreased in the Arcins channel with time. Immediately prior to the bore, the surface velocity dropped down to +0.2 to +0.3 m/s at the channel centre. The tidal bore passage had a marked effect on the velocity field, as seen in Fig. 5. This included a rapid flow deceleration and flow reversal, followed by large and rapid fluctuations of all velocity components during the early flood tide. Typical velocity data about the flow deceleration phase are illustrated in Fig. 5D. The maximum flow deceleration ranged from -0.65 m/s^2 to -1.4 m/s^2. The present observations were consistent with earlier field measurements with cruder instruments (e.g. rotor-type, electro-magnetic current meter, acoustic Doppler current profiler, acoustic tomography) (Lewis, 1972; Kjerfve and Ferreira, 1993; Navarre, 1995; Simpson et al., 2004; Wolanski et al., 2004; Bonneton et al., 2015; Furgerot et al., 2016; Kawanisi et al., 2017), albeit the present study had a much finer temporal resolution. A few field studies, based upon acoustic Doppler velocimetry (Mouaze et al., 2010; Chanson et al., 2011; Reungoat et al., 2014, 2015, Furgerot et al., 2016), documented comparable levels of flow deceleration during the bore passage and of velocity fluctuations during the early flood tide.

3.2. Suspended sediment processes

The time-variations of suspended sediment concentration estimate were deduced from the acoustic backscatter amplitude data. Typical data sets are presented in Fig. 6 together with the water depth, the longitudinal velocity data and the sediment concentrations of water samples collected on site and tested in laboratory afterwards. The data showed some low SSC estimates at the end of the ebb tide: that is, SSC <2 kg/m^3 typically (Appendix II). The water samples yielded SSC ≈3 kg/m^3 on average, immediately before the bore (Fig. 6B). The passage of the tidal bore was associated with a rapid increase in SSC levels together with large and rapid fluctuations in SSC estimates. After the bore, the water samples' colour was dark brown. During the flood tide, the SSC estimates tended to decrease, about 30–45 min after the bore passage. For all field studies, maximum SSC estimates were observed about 500–600 s after the bore passage, with maximum instantaneous SSC estimates up to 90–130 kg/m^3 (Appendix II), while the water sample analysis yielded maximum SSCs up to 67 kg/m^3 (Fig. 6-B).

The SSC estimate data indicated large sediment concentrations during the tidal bore and early flood tide (Fig. 6A). The result was consistent with the visual observations of murky water during the bore event and they were close to the water sample data, although the latter were collected closer to the water surface. The data were also comparable to earlier field observations (Chanson et al., 2011; Fan et al., 2012; Keevil et al., 2015; Furgerot et al., 2016). All water sample data are summarised in Fig. 6B, showing the water samples' SSC as a function of the relative time of passage of tidal bore on each collection day: i.e., t-T_{bore} = 0 at bore passage time in Fig. 6B.

The instantaneous suspended sediment flux per unit area q_s was calculated from the instantaneous velocity and SSC estimate data:

$$q_s = V_x \times SSC \tag{4}$$

with q_s and V_x positive in the downstream direction. Typical results are presented in Fig. 7. All the sediment flux data indicated a small downstream mass flux during the end of ebb tide (Fig. 7). On

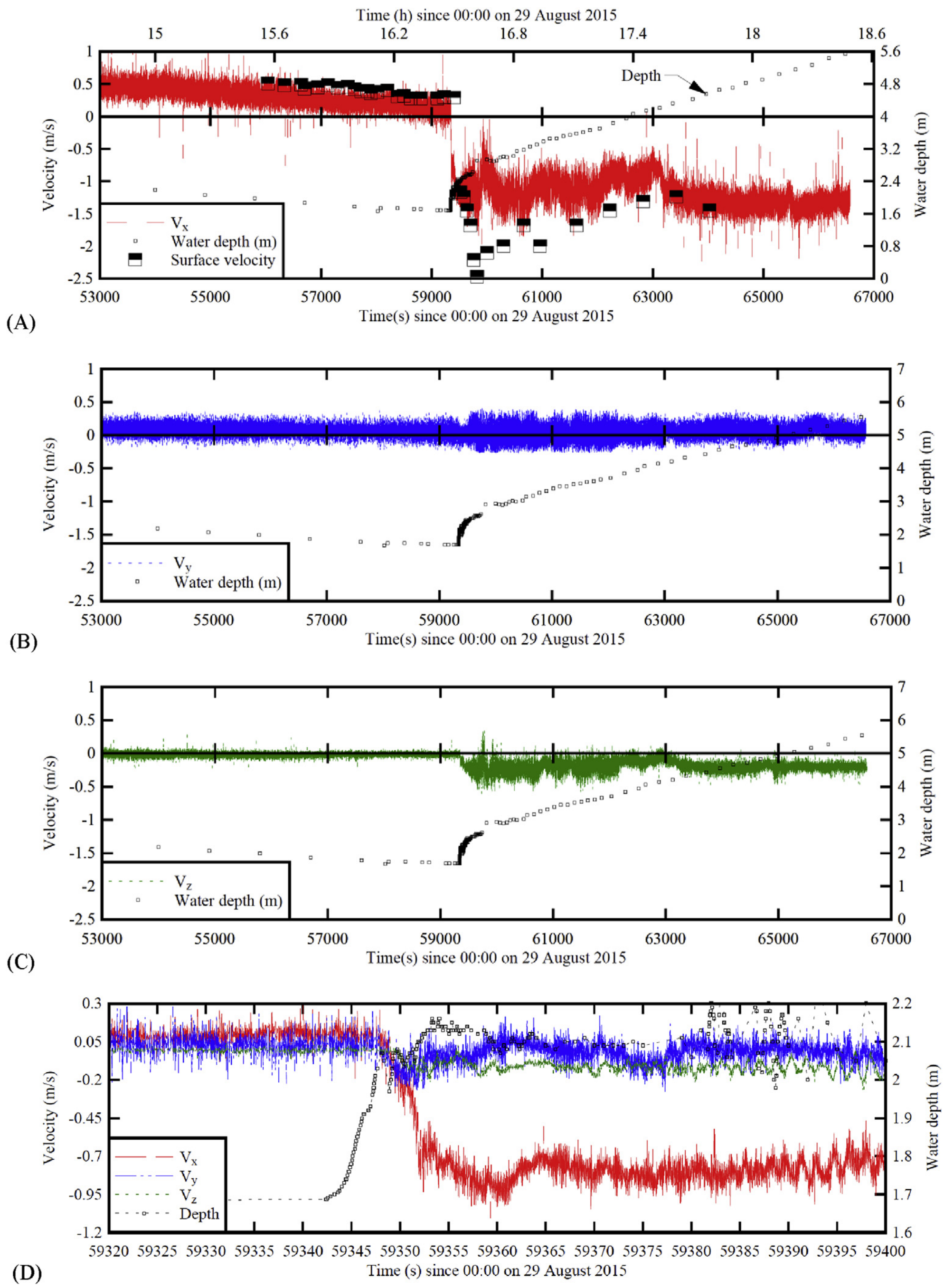

Fig. 5. Time-variations of water depth, surface velocity and instantaneous longitudinal, transverse and vertical velocity components (ADV data sampled at 200 Hz) during the tidal bore in the Arcins channel on 29 August 2015 - Entire data set (Fig. 5A and C) and details of tidal bore passage data (Fig. 5D).

average, the suspended sediment flux per unit area was less than 12.5 $kg/m^2/s$ prior to the tidal bore (Appendix II). The tidal bore passage was characterised by a sudden sediment flux reversal and a sharp increase in sediment flux magnitude during the early flood tide. The sediment flux data q_s presented also large and rapid fluctuations.

The suspended sediment flux data suggested further a two-stage bed erosion process (Fig. 7). During the bore passage, surface erosion occurred initially, in the form of stripping and aggregate fragmentation (Pouv et al., 2014; Keevil et al., 2015). The surface erosion took place because the fluid shear stresses exceeded the local strength of the bed, which was close to the apparent yield stress of the mud material (Van Kessel and Blom, 1998; Jacobs et al., 2011). The first stage was followed after some delay by mass erosion occurring rapidly (Amos et al., 1992; Pouv et al., 2014). In the Arcins channel, delayed bulk erosion occurred about 5–15 min after the tidal bore. For comparison, Pouv et al. (2014) observed bulk erosion about 7–40 min after the laboratory experiment start depending upon the experimental conditions. The two stage process is highlighted in Fig. 7 (black arrows). It is believed that the tidal bore propagation induced a massive shearing next to the bed surface, causing immediately some surface erosion, followed by delayed mass erosion. The process was consistent with the past and present observations of sediment upwelling and flocs bursting at

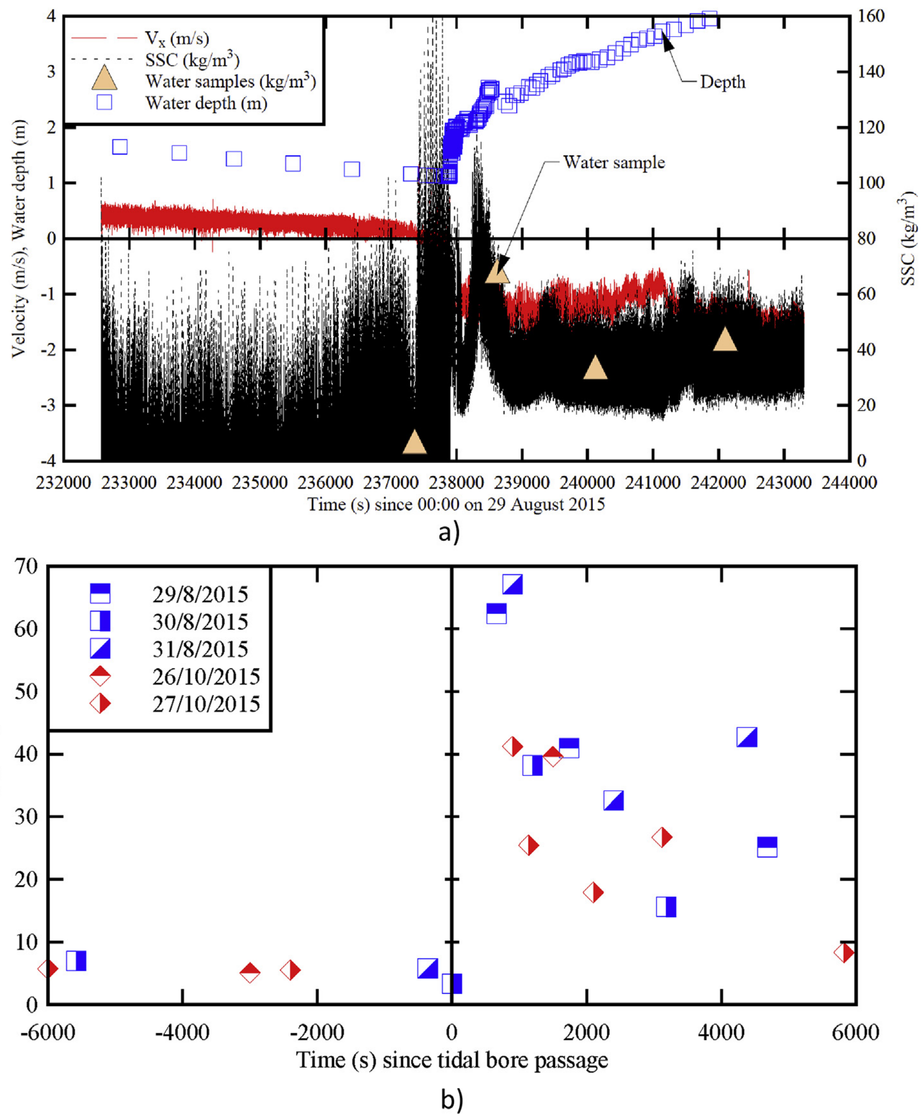

Fig. 6. Suspended sediment concentrations in the Arcins channel prior to, during and after the tidal bore passage in August and October 2015. (A) Time variation of water depth and SSC estimates in the Arcins channel, Garonne River on 31 August 2015 - Comparison with the sediment-laden water sample data. (B) Suspended sediment concentration of sediment-laden water samples collected at Arcins in August and October 2015 as a function of the relative time of passage of tidal bore on each collection day.

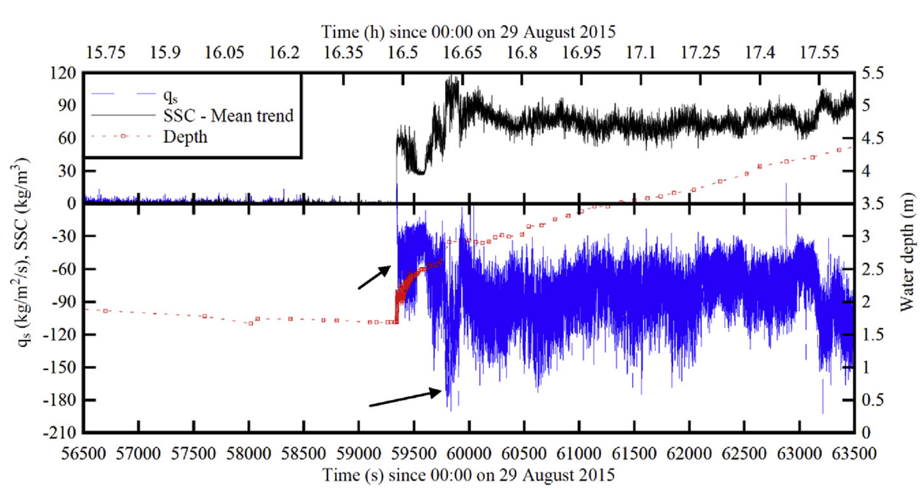

Fig. 7. Time variation of suspended sediment flux per unit area, low-pass filtered SSC estimates (VITA) and water depth in the Arcins channel, Garonne River on 29 August 2015 - Arrows point to initial surface erosion and delayed mass erosion.

the free-surface during the early flood tide.

Shortly after the bore passage, the instantaneous sediment flux per unit reached very large mean negative values up to −200 kg/m²/s (Appendix II). For the first 60 min of the early flood tide, the sediment flux was about −49 kg/m²/s on average for all 5 tidal bore events. The sediment flux data q_s were integrated with respect to time to yield the net sediment mass transfer per unit area during the first hour of the flood tide:

$$\int_{T_{bore}}^{T_{bore}+1h} V_x \times SSC \times dt \tag{5}$$

The results are summarised in Fig. 8 and detailed in Appendix II. The passage of the tidal bore and early flood tide induced a massive suspended sediment motion, advected upstream behind the bore. Assuming an uniform sediment flux across the Arcins channel, the time-averaged data for the first 3600 s would yield a mass transport of about 500 tonnes of sediments per second in the 70 m wide channel. The large sediment concentration and suspended sediment flux data in the Garonne River during and after the tidal bore implied that a significant length of the estuarine section of the Garonne River was affected and the tidal bore process would mobilise an enormous amount of sediments. The Garonne River experiences large variability in turbidity levels, with the occurrence of the turbidity maximum zone (TMZ) sensitive to changes in hydrological conditions (Jalon-Rojas et al., 2015). The tidal bore might contribute to some intensification of the TMZ occurrence in the fluvial Garonne.

4. Summary

The sediment analyses showed close results with past field measurements at the same site. These studies were conducted over one to two days, providing a snapshot based upon a single bore event. Herein new field measurements were repeated systematically at the same site on 29 August, 30 August, 31 August, 1 September and 27 October 2015. Between 29 August and 1 September, a careful characterisation of the sediment materials showed some temporal trend linked with the occurrence of tidal bore, first observed on 29 August.

The bed material granulometry data showed a progressively broader grain size distribution associated with some increase in median sediment size from day 1 to day 4. The apparent yield stress

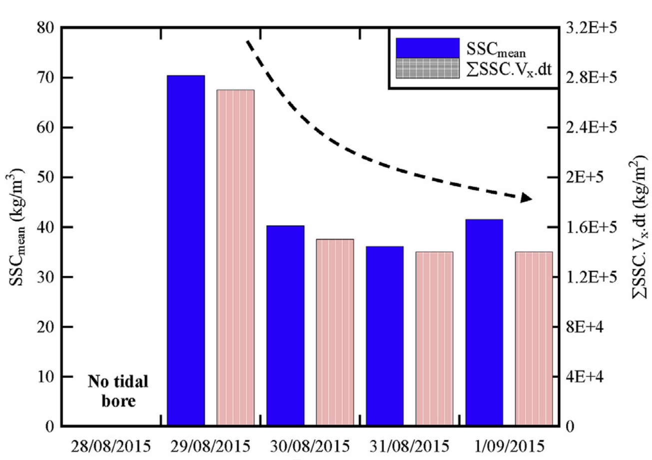

Fig. 8. Evolution of averaged SSC and suspended sediment flux per unit area during the first hour of the flood tide (following the tidal bore passage) in the Arcins channel, Garonne River between 29 August and 1 September 2015.

and effective viscosity of bed materials increased over the four days. It is suggested that the surface erosion during the tidal bore and early flood tide, and the subsequent deposition during the late flood tide and ebb tide, might have contributed to some mixing between different sediments sources, thus changing progressively the bed material characteristics between 29 August and 1 September 2015.

Very large SSC estimates were observed during and immediately after the passage of the tidal bore. Some substantially-large SSC estimate level was recorded during the early flood tide for the entire record durations, associated large fluctuations in SSC estimates during the same period. Between day 1 and day 4, a gradual increase in initial mean SSC estimate was recorded prior to the bore, which could be consistent with the thinner layer to sediment deposition on the river bank for the same period.

The suspended sediment flux was most significant on 29 August 2015: that is, on the first day of tidal bore occurrence. The suspended sediment flux tended to decrease from day 1 to day 4. The suspended sediment flux levels were larger in 2015 than in previous years, although any comparison between present and earlier data in the Arcins channel must be considered with great care, because of the differences in instrumentation and type of data (instantaneous versus average). The suspended sediment flux data suggested a two-stage bed scour process, with initially surface erosion followed by mass/bulk erosion.

Overall the present field study expanded largely the dataset of previous field studies by repeating continuous and consistent measurements over a consecutive number of days. The current data, while agreed in principle the key findings of the previous studies, demonstrated some novel and original insights into the sedimentary processes and impact of successive propagations of tidal bores over a period of four consecutive days: (a) Progressive change in bed material composition occurred due to the impact of successive bores, indicated by a gradually broader grain size distribution of the bed sediment, increases in apparent yield stress and effective viscosity as the days passed. (b) Thin layer of sediments was scoured, carried and then deposited upstream by the flood tide of the bore two times a day, resulting in a gradual increase in initial mean SSC every second day. (c) A key outcome is the massive suspended sediment transport recorded during the first hour of the ebb tide immediately after the tidal bore passage. During this period, both the time-averaged suspended sediment concentration and the suspended sediment mass per unit area were the largest on the first day of occurrence of the tidal bore, and tended to be lower in the following days. This finding was possibly counter-intuitive, since the tidal bore was the strongest (e.g. in terms of bore height) a couple of days later.

Acknowledgements

The authors thank Dr Frédérique LARRARTE (IFSTTAR Nantes, France), Professor Michele MOSSA (Politecnico di Bari, Italy), Dr Kyle STROM (Virginia Tech, USA), and Dr Emmanuel MIGNOT (INSA Lyon, France) for their initial comments. The authors acknowledge the assistance of Patrice BENGHIATI and the permission to access and use the pontoon in the Bras d'Arcins. They thank all the people who participated to the field works, and without whom the study could not have been conducted. They also thank Frédéric DANEY (Bordeaux, France) for a number of useful discussions and information. The authors acknowledge the financial assistance of the Agence Nationale de la Recherche (Projet Mascaret ANR-10-BLAN-0911), and they thank the project leader Prof. Pierre LUBIN (Université of Bordeaux, France), for his generous support and personal contribution to the field works.

Appendix I. Characteristics of bed and suspended sediment samples collected in the Garonne River between 29 August and 1 September 2015 - comparison with previous results

Reference	Sediment sampling date	Location	Type	d_{50}	d_{10}	d_{90}	$\sqrt{d_{90}/d_{10}}$	τ_c	μ	m
				μm	μm	μm		Pa	Pa.s	
(1)	(2)	(3)	(4)	(5)	(6)	(7)	(8)	(9)	(10)	(11)
Present study	29/08/2015	Garonne River in Arcins channel at low tide	Bed material	13.46	4.24	43.00	3.19	11.09	7.17	0.27
	30/08/2015			14.47	4.11	53.22	3.60	10.29	7.33	0.27
	31/08/2015			15.04	3.94	63.24	4.01	12.40	8.9	0.27
	01/09/2015			19.40	4.56	90.10	4.45	14.01	9.25	0.27
	27/10/2015			16.18	4.31	71.20	4.06	11.35	3.61	0.31
	29/08/2015 16:38	Garonne River in Arcins channel 0.1 m below water surface	Water samples	13.85	2.21	57.64	5.11	–	–	–
	29/08/2015 16:56			25.16	3.03	185.4	7.82	–	–	–
	29/08/2015 17:45			11.07	2.12	40.76	4.38	–	–	–
	30/08/2015 18:13			14.24	1.16	70.80	5.73	–	–	–
	26/10/2015 14:00			*8.97*	*2.32*	*26.10*	*3.35*	–	–	–
	26/10/2015 15:15			13.88	4.46	45.09	3.18	–	–	–
	27/10/2015 14:00			*9.12*	*2.23*	*26.80*	*3.46*	–	–	–
	27/10/2015 15:05			*9.13*	*2.31*	*27.25*	*3.43*	–	–	–
	27/10/2015 15:55			13.55	4.18	44.68	3.27	–	–	–
	27/10/2015 15:59			13.15	4.03	41.25	3.20	–	–	–
	27/10/2015 16:15			12.03	3.56	41.82	3.43	–	–	–
	27/10/2015 16:32			13.23	4.12	41.88	3.19	–	–	–
	27/10/2015 17:17			9.65	2.28	30.46	3.66	–	–	–
	28/10/2015 09:40			8.48	1.95	25.36	3.61	–	–	–
Keevil et al. (2015)	19/10/2013	Garonne River in Arcins channel at low tide	Bed material	15.06	4.13	56.93	3.715	5.93	4.48	0.28
Reungoat et al. (2014)	7/06/2012	Garonne River in Arcins channel at low tide	Bed material	12.22	3.07	48.66	3.975	173	26.8	0.31
	8/06/2012	Garonne River in Arcins channel at mid ebb tide	Bed material	13.24	3.63	51.29	3.75	37.1	9.1	0.38
Chanson et al. (2011)	11/09/2010	Garonne River in Arcins channel at low tide	Bed material	–	–	–	–	55.5	48.8	0.28

Notes: Grey shaded data: sediment suspension data; *Italic shaded data*: sediment suspension data prior to the tidal bore.

Appendix II. Suspended sediment concentration and flux in the Arcins channel, Garonne River immediately prior to, during and immediately after the tidal bore in 2015 - comparison with 2012 and 2013 observations

Flow property	Date						
	7/6/12	19/10/13	29/8/15	30/8/15	31/8/15	1/9/15	27/10/15
Froude number Fr_1	1.02	1.27	1.18	1.34	1.70	1.38	1.33
Initial flow conditions							
Initial water depth (m) ([1])	2.72	2.05	1.685	1.25	1.12	1.28	1.24
Initial $\overline{SSC}$ (kg/m^3) ([2])	34.1	2.4	0.4	1.6	–	0.3	0.7
Initial flux $\overline{q_s}$ (kg/m^2/s) ([2])	11.6	0.25	0.04	0.16	0.01	0	0.05
Very early flood tide (T_{bore}+20s)							
$\overline{SSC}$ (kg/m^3) ([2])	32.8	25.9	57.9	64.7	54.9	49.8	54.0
ssc' (kg/m^3)	2.49	–	8.25	7.24	7.66	7.51	8.64
$\overline{q_s}$ (kg/m^2/s)	−15.15	−20.5	−47.4	−53.8	−45.1	−41.8	−44.0
q_s' (kg/m^2/s)	1.58	–	8.54	8.97	6.68	7.14	7.84
Early flood tide							
SSC_{max} (kg/m^3) ([2])	47.5	59.3	128.9	93.0	130.5	107.1	94.9
Time after bore passage (s)	397	487	663	577	534	562	452
$(q_s)_{max}$ (kg/m^2/s)	***−33.1***	−73.4	−194.3	−152.0	−198.6	−131.1	−123.9
Time after bore passage (s)	–	457	616	248	534	529	134
Flood tide ($T_{bore} < t < T_{bore}$+3600s)							
$\overline{SSC}$ (kg/m^3) ([2])	31.7	31.55	68.0	38.5	35.6	40.5	25.9
$\int_{T_{bore}}^{T_{bore}+1hour} SSC \times V_x \times dt$ (kg/m^2)	-0.73×10^5	-0.80×10^5	-2.7×10^5	-1.5×10^5	-1.4×10^5	-1.4×10^5	-1.9×10^5

Notes: ([1]): at survey staff; ([2]): ADV data; Grey shaded data: OBS data (5 s average); ***Bold italic data***: suspicious data.

References

Amos, C.L., Daborn, G.R., Christian, H.A., Atkinson, A., Robertson, A., 1992. In situ erosion measurements on fine grained sediments from the Bay of Fundy. Mar. Geol. 108, 175–196. http://dx.doi.org/10.1016/0025-3227(92)90171-D.

Bartsch-Winkler, S., Emanuel, R.P., Winkler, G.R., 1985. Reconnaissance hydrology and suspended sediment analysis, turnagain arm estuary, upper cook Inlet. In: Bartsch-Winkler, S. (Ed.), The United States Geological Survey in Alaska; Accomplishments during 1984, pp. 49–51. U.S. Geological Survey Circular 967.

Bonneton, P., Bonneton, N., Parisot, J.P., Catelle, B., 2015. Tidal bore dynamics in funnel-shaped estuaries. J. Geophys. Res. Oceans 120, 923–941.

Brown, R., Chanson, H., 2012. Suspended Sediment Properties and Suspended Sediment Flux Estimates in an Urban Environment during a Major Flood Event, vol. 48. Water Resources Research, AGU, p. 15. http://dx.doi.org/10.1029/2012WR012381. Paper W11523.

Chanson, H., 2012. Momentum considerations in hydraulic jumps and bores. J. Irrigation drain. eng. ASCE 138 (4), 382–385. http://dx.doi.org/10.1061/(ASCE)IR.1943-4774.0000409.

Chanson, H., 2011. Tidal Bores, Aegir, Eagre, Mascaret, Pororoca: Theory and Observations. World Scientific, Singapore, p. 220 (ISBN 9789814335416).

Chanson, H., Jarny, S., Coussot, P., 2006. Dam break wave of thixotropic fluid. J. Hydraulic Eng. ASCE 132 (3), 280–293. http://dx.doi.org/10.1061/(ASCE)0733-9429(2006)132:3(280).

Chanson, H., Reungoat, D., Simon, B., Lubin, P., 2011. High-frequency turbulence and suspended sediment concentration measurements in the Garonne River tidal bore. Estuar. Coast. Shelf Sci. 95 (2–3), 298–306. http://dx.doi.org/10.1016/j.ecss.2011.09.012.

Chen, Jiyu, Liu, Cangzi, Zhang, Chongle, Walker, H.J., 1990. Geomorphological development and sedimentation in Qiantang estuary and hangzhou Bay. Jl Coast. Res. 6 (3), 559–572.

Coussot, P., 1997. Mudflow Rheology and Dynamics. IAHR Monograph, Balkema, The Netherlands.

Downing, A., Thorne, P.D., Vincent, C.E., 1995. Backscattering from a suspension in the near field of a piston transducer. J. Acoust. Soc. Am. 97 (3), 1614–1620.

Faas, R.W., 1995. Rheological constraints on fine sediment distribution and behavior: the cornwallis estuary, novia scotia. Proc. Can. Coast. Conf. Dartm. Nova Scotia 301–314.

Fan, D., Cai, G., Shang, S., Wu, Y., Zhang, Y., Gao, L., 2012. “Sedimentation processes and sedimentary characteristics of tidal bores along the north bank of the Qiantang Estuary. Chin. Sci. Bull. 57 (13), 1578–1589. http://dx.doi.org/10.1007/s11434-012-4993-6.

Fan, D., Tu, J., Shang, S., Cai, G., 2014. Characteristics of tidal-bore deposits and facies associations in the Qiantang Estuary, China. Mar. Geol. 348, 1–14. http://dx.doi.org/10.1016/j.margeo.2013.11.012.

Furgerot, L., Mouaze, D., Tessier, B., Perez, L., Haquin, S., 2013. Suspended Sediment Concentration in Relation to the Passage of a Tidal Bore (Sée River Estuary, Mont Saint Michel, NW France). Proc. Coastal Dynamics 2013, Arcachon, France, 24-28 June, pp. 671–682.

Furgerot, L., Mouaze, D., Tessier, B., Perez, L., Haquin, S., Weill, P., Crave, A., 2016. Sediment transport induced by tidal bores. An estimation from suspended matter measurements in the Sée River (Mont-Saint-Michel Bay, northwestern France). Comptes Rendus Geosci. 348, 432–441.

Greb, S.F., Archer, A.W., 2007. Soft-sediment deformation produced by tides in a Meizoseismic area, turnagain arm, Alaska. Geology 35 (5), 435–438.

Guerrero, M., Szupiany, R.N., Amsler, M., 2011. Comparison of acoustic backscattering techniques for suspended sediments investigation. Flow Meas. Instrum. 22, 392–401.

Ha, H.K., Hsu, W.Y., Maa, J.P.Y., Shao, Y.Y., Holland, C.W., 2009. Using ADV backscatter strength for measuring suspended cohesive sediment concentration. Cont. Shelf Res. 29, 1310–1316.

Jacobs, W., Le Hir, P., Van Kesteren, W., Cann, P., 2011. “Erosion threshold of sand–mud mixtures. Cont. Shelf Res. 31 (Suppl.), S14–S25. http://dx.doi.org/10.1016/j.csr.2010.05.012.

Jalon-Rojas, I., Schmidt, S., Sottolochio, A., 2015. Turbidity in the fluvial Gironde Estuary (southwest France) based on 10-year continuous monitoring: sensitivity to hydrological conditions. Hydrol. Earth Syst. Sci. 19, 2805–2819. http://dx.doi.org/10.5194/hess-19-2805-2015.

Julien, P.Y., 1995. Erosion and Sedimentation. Cambridge University Press, Cambridge, UK, p. 280.

Kawanisi, K., Zhu, X.H., Fan, X., Nistor, I., 2017. Monitoring tidal bores using acoustic tomographic system. J. Coast. Res. 33 (1), 96–104.

Keevil, C.E., Chanson, H., Reungoat, D., 2015. Fluid flow and sediment entrainment in the Garonne River bore and tidal bore collision. Earth Surf. Process. Landforms 40 (12), 1574–1586. http://dx.doi.org/10.1002/esp.3735.

Khezri, N., Chanson, H., 2012. Inception of bed load motion beneath a bore. Geomorphology 153–154, 39–47. http://dx.doi.org/10.1016/j.geomorph.2012.02.006.

Khezri, N., Chanson, H., 2015. Turbulent velocity, sediment motion and particle trajectories under breaking tidal bores: simultaneous physical measurements. Environ. Fluid Mech. 15 (3), 633–651. http://dx.doi.org/10.1007/s10652-014-9358-z. DOI: 10.1007/s10652-014-9360).

Kjerfve, B., Ferreira, H.O., 1993. Tidal bores: first ever measurements. Ciência e Cult. (Jl Braz. Assoc. Adv. Sci. 45 (2), 135–138. March/April.

Lambiase, J.J., 1980. Hydraulic control of grain-size distributions in a macrotidal estuary. Sedimentology 27, 433–446. http://dx.doi.org/10.1111/j.1365-3091.1980.tb01192.

Lewis, A.W., 1972. Field Studies of a Tidal Bore in the River Dee. M.Sc. thesis. Marine Science Laboratories, University College of North Wales, Bangor, UK.

Lighthill, J., 1978. Waves in Fluids. Cambridge University Press, Cambridge, UK, p. 504.

Mouaze, D., Chanson, H., Simon, B., 2010. Field Measurements in the Tidal Bore of the Sélune River in the Bay of Mont Saint Michel (September 2010). Hydraulic Model Report No. CH81/10. School of Civil Engineering, The University of Queensland, Brisbane, Australia, p. 72 (ISBN 9781742720210).

Navarre, P., 1995. Aspects Physiques du Caractère Ondulatoire du Macaret en Dordogne ('Physical Features of the Undulations of the Dordogne River Tidal Bore.') D.E.A. thesis. University of Bordeaux, France, p. 72 (in French).

Pouv, K.S., Besq, A., Gullou, S.S., Toorman, E.A., 2014. On cohesive sediment erosion: a first experimental study of the local processes using transparent model materials. Adv. Water Resour. 72, 71–83.

Reungoat, D., Chanson, H., Caplain, B., 2014. Sediment processes and flow reversal in the undular tidal bore of the Garonne River (France). Environ. Fluid Mech. 14 (3), 591–616. http://dx.doi.org/10.1007/s10652-013-9319-y.

Reungoat, D., Chanson, H., Keevil, C.E., 2015. Field measurements of unsteady turbulence in a tidal bore: the Garonne River in october 2013. J. Hydraulic Res. IAHR 53 (3), 291–301. http://dx.doi.org/10.1080/00221686.2015.1021717.

Reungoat, D., Leng, X., Chanson, H., 2016. Hydrodynamic and Sedimentary Processes of Tidal Bores: Arcins Channel, Garonne River in August-September-October 2015. Hydraulic Model Report No. CH102/16. School of Civil Engineering, The University of Queensland, Brisbane, Australia, p. 270.

Roussel, N., Le Roy, R., Coussot, P., 2004. Thixotropy modelling at local and macroscopic scales. Jl Newt. Fluid Mech. 117 (2–3), 85–95.

Salehi, M., Strom, K.B., 2009. Suspended sediment concentration measurements of muddy sediments with an ADV. In: Starrett, S. (Ed.), Proc. ASCE/EWRI World Water & Environmental Resources Congress, vol. 342. ASCE, Kansas City, MO, pp. 3572–3578.

Simpson, J.H., Fisher, N.R., Wiles, P., 2004. Reynolds stress and TKE production in an estuary with a tidal bore. Estuar. Coast. Shelf Sci. 60 (4), 619–627.

Stoker, J.J., 1957. Water Waves. The Mathematical Theory with Applications. Interscience Publishers, New York, USA, p. 567.

Tessier, B., Terwindt, J.H.J., 1994. An example of soft-sediment deformations in an intertidal environment - the effect of a tidal bore. Comptes-Rendus l'Académie Sci. Série II 319 (2), 217–233. Part 2 (in French).

Tricker, R.A.R., 1965. Bores, Breakers, Waves and Wakes. American Elsevier Publ. Co., New York, USA.

Van Kessel, T., Blom, C., 1998. Rheology of cohesive sediments: comparison between a natural and an artificial mud. J. Hydraulic Res. IAHR, 36 (4), 591–612.

Wolanski, E., Williams, D., Spagnol, S., Chanson, H., 2004. Undular tidal bore dynamics in the daly estuary, northern Australia. Estuar. Coast. Shelf Sci. 60 (4), 629–636.